Journal of Cellular Biochemistry

Essential Role of Lysophosphatidylcholine Acyltransferase 3 in the Induction of Macrophage Polarization in PMA-Treated U937 Cells

Journal:	*Journal of Cellular Biochemistry*
Manuscript ID:	Draft
Wiley - Manuscript type:	Research Article
Date Submitted by the Author:	n/a
Complete List of Authors:	Taniguchi, Kosuke; Kyushu Dental University, Division of Infections and Molecular Biology, Department of Health Promotion Hikiji, Hisako; Kyushu Dental University, Department of Oral Functional Management Okinaga, Toshinori; Kyushu Dental University, Division of Infections and Molecular Biology, Department of Health Promotion Hashidate-Yoshida, Tomomi; National Center for Global Health and Medicine, Department of Lipid Signaling, Research Institute Shindou, Hideo; National Center for Global Health and Medicine, Department of Lipid Signaling, Research Institute Ariyoshi, Wataru; Kyushu Dental University, Division of Infections and Molecular Biology, Department of Health Promotion Shimizu, Takao; National Center for Global Health and Medicine, Department of Lipid Signaling, Research Institute; The University of Tokyo, Department of Biochemistry and Molecular Biology (Lipidomics), Faculty of Medicine Tominaga, Kazuhiro; Kyushu Dental University, Division of Oral and Maxillofacial Surgery, Department of Science of Physical Function Nishihara, Tatsuji; Kyushu Dental University, Division of Infections and Molecular Biology, Department of Health Promotion
Keywords:	lysophosphatidylcholine acyltransferase 3, macrophage polarization, U937 cells

Essential Role of Lysophosphatidylcholine Acyltransferase 3 in the Induction of Macrophage Polarization in PMA-Treated U937 Cells

Kosuke Taniguchi,[1,2] Hisako Hikiji,[3]* Toshinori Okinaga,[1] Tomomi Hashidate-Yoshida,[4] Hideo Shindou,[4,5] Wataru Ariyoshi,[1] Takao Shimizu,[4,6] Kazuhiro Tominaga,[2] and Tatsuji Nishihara[1]

[1] Division of Infections and Molecular Biology, Department of Health Promotion, Kyushu Dental University, Kitakyushu, Fukuoka 803-8580, Japan

[2] Division of Oral and Maxillofacial Surgery, Department of Science of Physical Function, Kyushu Dental University, Kitakyushu, Fukuoka 803-8580, Japan

[3] Department of Oral Functional Management, Kyushu Dental University, Kitakyushu, Fukuoka 803-8580, Japan

[4] Department of Lipid Signaling, Research Institute, National Center for Global Health and Medicine, Tokyo 162-8655, Japan

[5] CREST, Japan Science and Technology Agency, Kawaguchi, Saitama 332-0012, Japan

[6] Department of Biochemistry and Molecular Biology (Lipidomics), Faculty of Medicine, The University of Tokyo, 113-0033, Japan

Running head: LPCAT3 regulates M1M2-macrophage polarization

* Correspondence to: Hisako Hikiji, D.D.S., Ph.D., Department of Oral Functional Management, Kyushu Dental University, 2-6-1 Manazuru, Kokurakita-ku, Kitakyushu,

Fukuoka 803-8580, Japan;

Tel: +81-93-582-1131;

Fax: +81-93-582-6000

[redacted]

Keywords:

- **lysophosphatidylcholine acyltransferase 3;**
- **macrophage polarization;**
- **U937 cells**

Total number of figures: 7

Total number of tables: 1

Grant information

Contract grant sponsor: Ministry of Education, Culture, Sports, Science and Technology of Japan; Contract grant number: 23390467 (H.H.), 23792149 (T.O.), 24659841 (T.N.), 24229003 (T.S.), 26460380 (H.S.), and 26870879 (T.H.-Y.)

Abbreviations

CXCL10, C-X-C motif ligand 10;

DMSO, dimethyl sulfoxide;

DPPC, dipalmitoyl-phosphatidylcholine;

ELISA, enzyme-linked immunosorbent assay;

ER, endoplasmic reticulum;

FBS, fetal bovine serum;

IFN-γ, interferon-γ;

IL-1β, interleukin-1β;

IL-1ra, interleukin-1 receptor antagonist;

IL-4, interleukin-4;

LC-MS, liquid chromatography-mass spectrometry;

LPC, lysophosphatidylcholine;

LPCATs, lysophosphatidylcholine acyltransferases;

LPLATs, lysophospholipid acyltransferases;

LPS, lipopolysaccharide;

NF-κB, nuclear factor-kappa-B;

PAPC, palmitoyl-arachidonoyl-phosphatidylcholine;

PC, phosphatidylcholine;

PDPC, palmitoyl-docosahexaenoyl-phosphatidylcholine;

PLPC, palmitoyl-linoleoyl-phosphatidylcholine;

PMA, phorbol 12-myristate 13-acetate;

POPC, palmitoyl-oleoyl-phosphatidylcholine;

SDS, sodium dodecyl sulfate;

siRNA, small interfering RNA;

TGF-β, transforming growth factor-β;

TNF-α, tumor necrosis factor-α.

Abstract

Lysophospholipid acyltransferases (LPLATs) regulate the diversification of fatty acid composition in biological membranes. Lysophosphatidylcholine acyltransferases (LPCATs) are members of the LPLATs that play a role in inflammatory responses. M1 macrophages differentiate in response to lipopolysaccharide (LPS) and are pro-inflammatory, whereas M2 macrophages, which differentiate in response to interleukin-4 (IL-4), are anti-inflammatory and involved in homeostasis and wound healing. In the present study, we showed that LPCATs play an important role in M1/M2-macrophage polarization. LPS changed the shape of PMA-treated U937 cells from rounded to spindle shaped and upregulated the mRNA and protein expression of the M1 macrophage markers CXCL10, TNF-α, and IL-1β. IL-4 had no effect on the shape of PMA-treated U937 cells and upregulated the M2 macrophage markers CD206, IL-1ra, and TGF-β in PMA-treated U937 cells. These results suggest that LPS and IL-4 promote the differentiation of PMA-treated U937 cells into M1- and M2-polarized macrophages, respectively. LPS significantly downregulated the mRNA expression of LPCAT3, one of four LPCAT isoforms, and suppressed its enzymatic activity toward linoleoyl-CoA and arachidonoyl-CoA in U937 cells. LPCAT3 knockdown induced a spindle-shaped morphology typical of M1-polarized macrophages, and increased the secretion of CXCL10 and decreased the levels of CD206 in IL-4-activated U937 cells. This indicates that knockdown of LPCAT3 shifts the differentiation of PMA-treated U937 cells from M2- to M1-polarized macrophages. Our findings suggest that LPCAT3 plays an important role in M1/M2-macrophage polarization, providing novel potential therapeutic targets for the regulation of immune and inflammatory disorders.

Introduction

Glycerophospholipids are the major phospholipids in biological membranes and play an important role as the precursors of lipid mediators, including eicosanoids (Ishibashi et al., 2013), lysophospholipids (Kremer et al., 2010) and platelet-activating factor (PAF) (Snyder, 1989) (Ishii and Shimizu, 2000) in the inflammatory response. Glycerophospholipids are synthesized from glycerol-3-phosphate in the *de novo* pathway (Kennedy pathway) (Kennedy and Weiss, 1956) and mature in the remodeling pathway called Lands' cycle (Lands, 1958). In these processes, the recently identified lysophospholipid acyltransferases (LPLATs) play a major role in the configuration of the cellular membrane (Shindou et al., 2009) (Harayama et al., 2014). Through these pathways, phospholipids acquire diversity and asymmetry (sn-1 vs sn-2) by reacylation and deacylation reactions catalyzed by LPLATs and phospholipases A_2s, respectively.

Lysophosphatidylcholine acyltransferases (LPCATs), which are members of LPLATs, are localized in the endoplasmic reticulum (ER) of many cell types and incorporate various fatty acids into the *sn*-2 position of lysophosphatidylcholine (LPC) to produce phosphatidylcholine (PC). Four LPCATs (LPCAT1–4) have been identified and functionally characterized to date (Shindou et al., 2009) (Hishikawa et al., 2014). Several studies have shown that LPCATs exert various biological functions. LPCAT1, which selectively incorporates palmitoyl-CoA into LPC as a substrate in addition to its involvement in pulmonary surfactant production (Harayama et al., 2014; Nakanishi et al., 2006), affects the progression of hepatocellular carcinoma (Morita et al., 2013). LPCAT2 is activated by lipopolysaccharides (LPS) and produces the inflammatory lipid mediator PAF in mouse peritoneal macrophages (Shindou et al., 2007). LPCAT3, which

preferably incorporates linoleoyl-CoA and arachidonoyl-CoA into LPC (Hishikawa et al., 2008) (Zhao et al., 2008) (Kazachkov et al., 2008) , upregulates the expression of peroxisome proliferator-activated receptor γ (PPARγ) and might be associated with adipocyte differentiation (Eto et al., 2012). The liver X receptors (LXRs)-LPCAT3 pathway is an important modulator of inflammation (Rong et al., 2013). LPCAT4 is involved in the deregulation of PC in colorectal cancer (Kurabe et al., 2013).

Macrophages are divided into at least two main classes known as M1 and M2 (Solinas et al., 2009). When macrophages are exposed to LPS or interferon-γ (IFN-γ), they are polarized into M1 macrophages (Mosmann and Coffman, 1989), whereas exposure to interleukin-4 (IL-4) or IL-13 polarizes the cells into M2 macrophages (Abramson and Gallin, 1990). M1-polarized macrophages produce pro-inflammatory cytokines and chemokines, such as tumor necrosis factor-α (TNF-α), interleukin-1β (IL-1β), and C-X-C motif ligand 10 (CXCL10), and infiltrate into injured tissue soon after damage (Arnold et al., 2007). M2-polarized macrophages, whose markers are CD206, interleukin-1 receptor antagonist (IL-1ra), and transforming growth factor-β (TGF-β), are major resident macrophages and appear during the late stages of tissue repair and remodeling in injured tissue (Biswas and Mantovani, 2012)

Macrophages can switch from M1 to M2 or from M2 to M1 phenotypes according to their microenvironment or in response to certain stimuli (Biswas and Mantovani, 2012; Gordon and Martinez, 2010; Sica and Mantovani, 2012; Zhang et al., 2015). Several mechanisms of M1/M2-macrophage polarization have been reported. The transcription factor nuclear factor-kappa-B (NF-κB) is a key player in M1/M2-macrophage polarization (Biswas and Lewis, 2010). M2-polarized macrophages are epigenetically regulated by histone H3 lysine-4 and histone H3 lysine-27

methylation (Ishii et al., 2009). PPARγ promotes the differentiation of human monocytes to M2-polarized macrophages (Bouhlel et al., 2007). We speculated that M1/M2-macrophage polarization might be associated with LPCATs, as LPCATs and M1/M2-polarized macrophages play important roles in inflammatory responses. The relationship between LPCATs and M1/M2-macrophage polarization has not been reported to date.

In the present study, we investigated the physiological role of LPCAT3 in M1/M2-macrophage polarization and the underlying mechanism using human U937 cells. LPCAT3 mRNA expression was downregulated in LPS-activated U937 cells. Knockdown of LPCAT3 in U937 cells resulted in a shift from M2- to M1-polarized macrophages. Our results suggest that LPCAT3 exerts important anti-inflammatory effects mediated by the suppression of M1-macrophage polarization.

Materials and methods

Reagents

Recombinant human IL-4 was purchased from R&D Systems (Minneapolis, MN, USA). LPS from *Escherichia coli* 0111:B4 and phorbol 12-myristate 13-acetate (PMA) were purchased from Sigma-Aldrich (St. Louis, MO, USA). Antibodies and their respective sources were as follows: anti-IL-1β monoclonal antibody (Cell Signaling, Beverly, MA, USA), anti-CD206 polyclonal antibody (R&D Systems), anti-IL-1ra monoclonal antibody (Santa Cruz Biotechnology, Dallas, TX, USA), anti-β-actin monoclonal antibody (Sigma Aldrich), anti-goat IgG (Santa Cruz Biotechnology), anti-mouse IgG (GE Healthcare, Little Chalfont, UK). Deuterium-labeled 16:0 LPC, 16:0-, 18:1-, 18:2-, 20:4-, 22:6-CoA and dilauryl-PC were purchased from Avanti Polar Lipid (Alabaster, AL, USA).

Cell culture and differentiation

Human monocytic leukemia U937 cells (RIKEN, RCB0435) were cultured at 37°C in a humidified atmosphere of 5% CO_2 in RPMI 1640 supplemented with 10% heat-inactivated fetal bovine serum (FBS), 100 units/ml penicillin and 100 μg/ml streptomycin. U937 cells were seeded at a density of 5×10^5 cells/well into 6-well plates with RPMI1640 containing 5% FBS and 100 ng/ml PMA. After 12 h of culture, the cells were washed with phosphate-buffered saline (PBS, pH 7.2) and incubated with LPS (100 ng/ml) or IL-4 (20 ng/ml) for the indicated times.

Morphological characterization and quantification

Images of cells were acquired by phase-contrast microscope (Olympus IX71, Tokyo, Japan). Cells were washed with PBS and further cultured in RPMI 1640 containing 5% FBS for 72 h. The quantification of morphological changes was performed based on the criteria used in the analysis of neurite outgrowth (Shea and Beermann, 1994). Cells with more than twice the ratio of major axis to minor axis were defined as spindle-shaped cells. Spindle-shaped cells were counted in three randomly selected fields of triplicate cultures. Data are presented as a percentage of the total number of cells in the field.

Quantitative real-time reverse transcription polymerase chain reaction (RT-PCR)

Total cellular RNA was extracted with an RNeasy® Mini Kit (Qiagen, Valencia, CA, USA), according to the manufacturer's instructions. cDNA was synthesized with q-Script™ cDNA SuperMix reagents (Quanta BioSciences, Gaitherburg, MD, USA). qRT-PCR analysis was performed by StepOne™ Real-Time PCR Systems (Applied Biosystems, Foster City, CA, USA). The reaction for each gene was performed using Fast SYBR® Green Master Mix (Applied Biosystems). Relative quantification was calculated as a ratio of gene expression to the reference housekeeping gene, 18S rRNA. The sequences of the primer pairs used in this analysis are presented in Table 1.

Phagocytosis assay

Macrophage phagocytic activity was quantified using a Phagocytosis Assay Kit, IgG FITC (Cayman Chemical, Ann Arbor, MI, USA). Briefly, cells were seeded into 6-well plates at a density of 5×10^5 cells/well and treated with PMA (100 ng/ml) for 12 h. The cells were washed twice with PBS and stimulated with LPS or IL-4. After 48 h

of culture, 100 µl of the latex beads-rabbit IgG-FITC solution was added to each well. The cells were incubated for 24 h and then washed twice with PBS to remove the latex beads. All cells were analyzed using an EPICS XL (Beckman Coulter, Fullerton, CA, USA). Flow cytometric measurement was performed in the FL-1 channel.

Flow cytometry

PMA-treated U937 cells (5×10^5 cells) were cultured with IL-4 (20 ng/ml) for 72 h. After washing with PBS supplemented with 1% heat-inactivated FBS and 0.01% NaN_3, cells were resuspended in PBS. Cells were then incubated in Clear Back (human Fc receptor blocking reagent) (MBL, Nagoya, Japan) for 10 min followed by incubation with FITC-Mouse Anti-Human CD206 (BD Biosciences) for 30 min at room temperature in the dark. After the final washing step, labeled cells were analyzed by flow cytometry.

Western blot analysis

Cells were lysed in sodium dodecyl sulfate (SDS) buffer (50 mM Tris-HCl, 2% SDS; pH 6.8), and the protein concentration of the lysate was measured using a DC-protein assay kit (Bio-Rad, Hercules, CA, USA). Lysates were boiled at 95°C for 5 min in SDS loading buffer. Electrophoretic separation (10–25 µg protein/lane) was carried out on 7.5–15% polyacrylamide gels and then proteins transferred to PVDF membranes (Millipore, Bedford, MA, USA). The membranes were blocked for 30 min at room temperature with Blocking One (NACALAI TESQUE, Inc., Kyoto, Japan) and incubated overnight at 4°C with 0.1% Tween-20 in PBS (PBS-T) containing the primary antibody. After washing with PBS-T, the membranes were coated with

secondary antibody in PBS for 1 h at room temperature. After washing the membranes with PBS-T, chemiluminescence detection was performed using ECL reagent (Amersham Pharmacia Biotech, Uppsala, Sweden). Results were visualized using a Molecular Imager® ChemiDoc™ XRS Plus system (Bio-Rad). Densitometric analysis of protein bands was performed using Image Lab® (Bio-Rad, Munich, Germany). Relative expression was calculated by dividing the band intensities of the proteins of interest by that of β-actin.

Enzyme-linked immunosorbent assay (ELISA)

PMA-treated U937 cells (5×10^5 cells) were cultured with or without LPS (100 ng/ml) or IL-4 (20 ng/ml). The supernatants from stimulated U937 cells were collected at 72 h. The concentrations of CXCL10, TNF-α and TGF-β in the culture supernatants were determined using an ELISA kit (R&D systems) according to the manufacturer's instructions.

Protein preparation and measurement of LPCAT activity

U937 cells were scraped into 1 ml of ice-cold buffer containing 20 mM Tris-HCl (pH 7.4), 300 mM sucrose, and proteinase inhibitor cocktail (Complete, Roche, Basel, Switzerland). The cells were sonicated on ice three times for 30 seconds using a probe sonicator (Ohtake Works, Tokyo, Japan). After centrifugation at 9,000 × *g* for 10 min, the supernatants were centrifuged at 100,000 × *g* for 1 h. Resultant pellets were suspended in buffer containing 20 mM Tris-HCl (pH 7.4), 300 mM sucrose, and 1 mM EDTA, and protein concentration was measured using the Bio-Rad Protein Assay (Bio-Rad) with bovine serum albumin as a standard. LPCAT activity was measured

according to Harayama et al. (Harayama et al., 2014). Briefly, 0.01 μg protein was added to equal volumes of reaction mixtures containing 200 mM Tris-HCl (pH 7.4), 4 mM $CaCl_2$, 2 mM EDTA, 0.03% Tween-20 (Wako Pure Chemical Industries, Osaka, Japan), 2 μM each of 16:0-CoA, 18:1-CoA, 18:2-CoA, 20:4-CoA, and 22:6-CoA, and 50 μM deuterium labeled 16:0 LPC in a total volume of 0.1 ml. After incubation at 37°C for 10 min, reactions were stopped by the addition of 0.3 ml of chloroform:methanol (1:2, vol/vol) containing dilauryl-phosphatidylcholine as an internal standard. Total lipids were extracted by the method of Bligh and Dyer (Bligh and Dyer, 1959) and measured by an Acquity ultra performance liquid chromatography system (Waters, Milford, MA, USA) and a TSQ Vantage triple stage quadrupole mass spectrometer (Thermo Fisher Scientific, Waltham, MD, USA) (LC-MS).

Small interfering RNA transfection

Small interfering RNA (siRNA) targeting was used to knockdown LPCAT3 expression in U937 cells. siRNA against human LPCAT3 and siRNA control were purchased from Santa Cruz Biotechnology. LPCAT3 siRNA consisted of a pool of three target-specific 19–25 nt siRNAs designed to knock down gene expression. U937 cells were transfected using Lipofectamine® RNAi MAX (Invitrogen, Carlsbad, CA, USA) according to the manufacturer's instructions. In brief, cells (5×10^5 cells/well) were seeded into 6-well plates in 2 ml of RPMI supplemented with 5% FBS and treated with PMA (100 ng/ml) for 12 h. After washing with PBS, the cells were resuspended in 2 ml of RPMI supplemented with 5% FBS. Lipofectamine® RNAi MAX was first diluted in Opti-MEM (150 μl; Invitrogen) for 5 min before mixing with an equal volume of Opti-MEM containing the siRNA (12.5 nM). After 20 min of incubation, 250 μl of the

resulting RNAiMAX/siRNA was added directly onto the cells. After 24 h of incubation at 37°C (5% CO_2 atmosphere), the cells were rinsed with 2 ml of RPMI supplemented with 5% FBS and treated with IL-4 (20 ng/ml).

Statistical analysis

Statistical analyses were performed using Student's t test (two groups) or ANOVA (> two groups) followed by post hoc tests, the Tukey-Kramer test. A P value of < 0.05 was considered statistically significant. All statistical calculations were performed using EZR (Easy R, Saitama Medical Center, Saitama, Japan; http://www.jichi.ac.jp/saitama-sct/SaitamaHP.files/statmedEN.html), which is based on R and R commander (Kanda, 2013).

Results

PMA promotes the differentiation of human U937 monocytic cells into macrophage-like cells

Human U937 monocytic cells are non-adherent cells. After treatment with PMA (100 ng/ml) for 12 h, U937 cells attached to the culture dish and developed elongated projections (Fig. 1A). PMA treatment significantly increased the mRNA expression of the macrophage marker CD68 (Fig. 1B) and the phagocytic activity compared with those of DMSO-treated U937 cells (Fig. 1C). These results suggest that PMA promotes the differentiation of U937 cells into macrophage-like cells.

LPS promotes the differentiation of PMA-treated U937 cells into M1-polarized macrophages

LPS changed the shape of PMA-treated U937 cells from rounded to spindle-shaped (Fig. 2A, *upper left*), whereas IL-4 had no effect (Fig. 2A, *upper right*). LPS-activated U937 cells showed a significantly higher proportion of spindle-shaped cells than IL-4-activated U937 cells (Fig. 2A, *lower*). LPS promoted the phagocytic activity of PMA-treated U937 cells, whereas IL-4 had no effect (Fig. 2B). These results suggest that PMA-treated U937 cells themselves seem to be polarized into M2-polarized macrophages and that LPS may induce M1-polarized macrophages in PMA-treated U937 cells.

LPS upregulated the mRNA expression of the M1 markers CXCL10, TNF-α, and IL-1β at 12–24 h in PMA-treated U937 cells (Fig. 3A–C, *left*), increased the secretion of CXCL10 and TNF-α (Fig. 3A and B, *right*), and upregulated the protein

expression of IL-1β at 12–72 h (Fig. 3C, *right*). These results indicate that LPS promoted M1-polarization of macrophages in PMA-treated U937 cells.

In PMA-treated U937 cells, which show certain properties of M2-polarized macrophages, IL-4 upregulated the mRNA expression of the M2 markers CD206, IL-1ra, and TGF-β at 24–72 h (Fig. 4A–C, *left*), and upregulated the protein expression of CD206 and IL-1ra (Fig. 4A, *middle* and 4B, *right*). Flow cytometric analysis showed that IL-4-activated U937 cells expressed the surface marker CD206 (Fig. 4A, *right*). However, IL-4 did not affect the secretion of TGF-β (Fig. 4C, *right*), indicating that IL-4 increased expression of M2-markers, not all, in PMA-treated U937 cells. These results suggest that IL-4 enhanced M2-polarization in PMA-treated U937 cells, which were in nature M2-polarized macrophages.

LPS downregulates LPCAT3 in PMA-treated U937 cells

The gene expression profiles of LPCATs in LPS or IL-4-activated U937 cells were examined by real time qRT-PCR. LPS significantly downregulated the mRNA expression of LPCAT1, LPCAT2, and LPCAT3 at 12–72 h and that of LPCAT4 at 12 h in PMA-treated U937 cells (Fig. 5A). The LPS-induced downregulation of LPCAT2 in U937 cells differed from the previously-reported upregulation of LPCAT2 by LPS in mouse peritoneal macrophages; this discrepancy could be due to differences between the U937 cell line and primary macrophages. LPCAT3 mRNA expression in LPS-activated cells was reduced to one-tenth of that in untreated cells. IL-4 treatment caused a mild upregulation of LPCAT1 and LPCAT3 mRNA expression at 24–48 h and of LPCAT4 at 24 h. LPS significantly decreased LPCAT activity toward linoleoyl-CoA and arachidonoyl-CoA, whereas IL-4 did not (Fig. 5B). Neither LPS nor IL-4 changed

LPCAT activity toward palmitoyl-CoA, oleoyl-CoA, and docosahexaenoyl (DHA)-CoA.

Knockdown of LPCAT3 in PMA-treated U937 cells decreases LPCAT activity toward linoleoyl-CoA and arachidonoyl-CoA

PMA-treated U937 cells were transfected with control siRNA or LPCAT3 siRNA. Transfection of LPCAT3 siRNA into PMA-treated U937 cells efficiently downregulated the mRNA expression of LPCAT3 compared with the control siRNA (Fig. 6A). LPCAT activities toward linoleoyl-CoA and arachidonoyl-CoA were significantly decreased in LPCAT3 siRNA-transfected cells (Fig. 6B).

Knockdown of LPCAT3 shifts polarization from M2 to M1 in PMA-treated U937 cells

LPCAT3 siRNA-transfected cells showed a spindle-shaped morphology similar to that of M1-polarized macrophages, whereas control siRNA-transfected cells showed a rounded morphology typical of M2-polarized macrophages (Fig. 7A, *left*). LPCAT3 siRNA-transfected cultures had a significantly higher proportion of spindle-shaped cells than control siRNA-transfected cultures (Fig. 7A, *right*). Analysis of the mRNA and protein expression of the M1/M2 markers CXCL10 and CD206, which showed the highest expression among the investigated markers, indicated that LPCAT3 knockdown significantly increased the secretion of CXCL10, even after the IL-4 induced complete polarization of PMA-treated U937 cells into M2 macrophages at 48 h (Fig. 7B). Knockdown of LPCAT3 suppressed the IL-4 induced upregulation of CD206 protein expression (Fig. 7C). These results suggest that knockdown of LPCAT3 shifts

PMA-treated U937 cells from M2- to M1-polarized macrophages.

Discussion

M1- and M2-polarized macrophages are distinguished by their cellular morphology (Pelegrin and Surprenant, 2009; Zhang et al., 2015), surface antigen presentation, production of cytokines and chemokines (Biswas et al., 2006; Umemura et al., 2008), and phagocytic activity (Vereyken et al., 2011). CXCL10, TNF-α, and IL-1β are known to be released by M1-polarized macrophages and are referred to as M1-markers (Martinez et al., 2006; Muller-Quernheim et al., 2012). The macrophage mannose receptor CD206, IL-1ra, and TGF-β are anti-inflammatory and M2-macrophage markers. The mRNA and protein expression of CD206 is well known to be potently upregulated by IL-4 stimulation (Porcheray et al., 2005; Stein et al., 1992). However, some studies described that CD206 was not always good marker for human M2-macrophages (Daigneault et al., 2010; Jaguin et al., 2013). To confirm that CD206 is a proper marker of M2-polarized macrophages, we examined the surface expression of CD206 in IL-4-activated U937 cells by flow cytometry (Fig. 4A, *right*). Our results certainly showed that IL-4 increased the expression of CD206 in PMA-treated U937 cells.

A previous study suggested that the M1/M2-polarization pattern depends on the characteristics of the tissue microenvironment in U937 cells (Sanchez-Reyes et al., 2014). In the present study, we showed that PMA-treated U937 cells stimulated with LPS and IL-4 are fully polarized to M1- and M2-macrophages, respectively, indicating that M1/M2-macrophage polarization in U937 cells may be a useful model for the investigation of macrophage function. Human monocytic THP-1 cells are reported to differentiate into M2-polarized macrophages in response to PMA treatment (Tjiu et al.,

2009). In the present study, PMA-treated U937 cells showed low levels of CXCL10, TNF-α, and IL-1β and the typical cellular morphology and phagocytic activity of M2-polarized macrophages. These results suggest that PMA-treated U937 cells, which are in nature polarized toward M2-macrophages, fully shift into M2-polarized macrophages in response to IL-4.

Accumulation of saturated fatty acids, such as palmitic acid, causes lipotoxicity and induces inflammation, ER stress, and cell death (Ariyama et al., 2010; Prieur et al., 2011). By contrast, polyunsaturated fatty acids, such as linoleic acid, arachidonic acid and docosahexaenoic acid, reduce inflammation and ER stress induced by palmitic acid (Ishiyama et al., 2011; Rong et al., 2013). Furthermore, saturated fatty acids induce the expression of M1 markers, whereas polyunsaturated fatty acids strongly induce the expression of M2 markers in adipose tissue macrophages (Prieur et al., 2011). Sphingolipids, which are one of the essential lipid components of cellular membranes, regulate the differentiation of monocytes into macrophages in U937 cells (Yamamoto et al., 2011). LPCAT3 is reported to be a major contributor to increase polyunsaturated fatty acids, including linoleic acid and arachidonic acid, and is associated with inflammatory responses in human primary macrophages (Ishibashi et al., 2013). Therefore, among various LPCATs, LPCAT3 may particularly affect M1/M2-macrophage polarization associated with inflammation. In the present study, we showed that LPCAT3 mRNA expression was strongly downregulated and LPCAT activity toward linoleoyl-CoA and arachidonoyl-CoA was reduced in M1-polarized macrophages (Fig. 5).

Induction of LPCAT3 activity increases the abundance of polyunsaturated PCs and downregulates the expression of inflammatory mediators such as CXCL10, TNF-α,

and IL-1β in mouse primary macrophages. By contrast, knockdown of LPCAT3 decreases the abundance of polyunsaturated PCs and induces inflammatory responses (Rong et al., 2013). We showed that knockdown of LPCAT3 significantly increased the secretion of the M1 macrophage marker CXCL10 in PMA-treated U937 cells and M2-polarized macrophages. In addition, knockdown of LPCAT3 suppressed the expression of the M2 macrophage marker CD206, even after full M2-polarization by IL-4 (Fig. 7). Our results suggest that knockdown of LPCAT3 induces a phenotypic shift from M2- to M1-polarized macrophages.

Polyunsaturated fatty acids increase membrane fluidity and the flexibility of cellular membranes (Holzer et al., 2011), whereas excessive contents of saturated fatty acids reduce membrane fluidity. The decrease in the content of PCs containing linoleic acid or arachidonic acid in biological membranes caused by the suppression of LPCAT3 may influence membrane fluidity, curvature and function. In fact, LPCAT3 knockdown in HEK293 cells was reported to have a remarkable effect on cell morphology (Jain et al., 2009). Therefore, LPCAT3 induced alterations may also cause morphological changes, such as those of M1-polarized macrophages, in LPCAT3 siRNA-transfected cells.

In summary, we showed that modulation of LPCAT3 expression regulates M1-macrophage polarization. This study supports the development of new anti-inflammatory drugs capable of altering macrophage phenotypes via the remodeling pathway of glycerophospholipids.

Acknowledgments

This study was supported by JSPS KAKENHI Grant Numbers 23390467 (H.H.), 23792149 (T.O.), 24659841 (T.N.), 24229003 (T.S.), 26460380 (H.S.), and 26870879 (T.H.-Y.); CREST, JST (H.S.). The Department of Biochemistry and Molecular Biology (Lipidomics), Faculty of Medicine, The University of Tokyo, is financially supported by Shimadzu Corp. and Ono Pharmaceutical Co., Ltd.

References

Abramson SL, Gallin JI. 1990. IL-4 inhibits superoxide production by human mononuclear phagocytes. the Journal of Immunology 144(15):625-630.

Ariyama H, Kono N, Matsuda S, Inoue T, Arai H. 2010. Decrease in membrane phospholipid unsaturation induces unfolded protein response. The Journal of biological chemistry 285(29):22027-22035.

Arnold L, Henry A, Poron F, Baba-Amer Y, van Rooijen N, Plonquet A, Gherardi RK, Chazaud B. 2007. Inflammatory monocytes recruited after skeletal muscle injury switch into antiinflammatory macrophages to support myogenesis. The Journal of experimental medicine 204(5):1057-1069.

Biswas SK, Gangi L, Paul S, Schioppa T, Saccani A, Sironi M, Bottazzi B, Doni A, Vincenzo B, Pasqualini F, Vago L, Nebuloni M, Mantovani A, Sica A. 2006. A distinct and unique transcriptional program expressed by tumor-associated macrophages (defective NF-κB and enhanced IRF-3/STAT1 activation). Blood 107(5):2112-2122.

Biswas SK, Lewis CE. 2010. NF-κB as a central regulator of macrophage function in tumors. Journal of leukocyte biology 88(5):877-884.

Biswas SK, Mantovani A. 2012. Orchestration of metabolism by macrophages. Cell metabolism 15(4):432-437.

Bligh EG, Dyer WJ. 1959. A rapid method of total lipid extraction and purification. Can J Biochem Physiol 37(8):911-917.

Bouhlel MA, Derudas B, Rigamonti E, Dievart R, Brozek J, Haulon S, Zawadzki C, Jude B, Torpier G, Marx N, Staels B, Chinetti-Gbaguidi G. 2007. PPARγ activation primes human monocytes into alternative M2 macrophages with anti-inflammatory properties. Cell metabolism 6(2):137-143.

Daigneault M, Preston JA, Marriott HM, Whyte MK, Dockrell DH. 2010. The identification of markers of macrophage differentiation in PMA-stimulated THP-1 cells and monocyte-derived macrophages. PLoS One 5(1):e8668.

Eto M, Shindou H, Koeberle A, Harayama T, Yanagida K, Shimizu T. 2012. Lysophosphatidylcholine acyltransferase 3 is the key enzyme for incorporating arachidonic acid into glycerophospholipids during adipocyte differentiation. International journal of molecular sciences 13(12):16267-16280.

Gordon S, Martinez FO. 2010. Alternative activation of macrophages: mechanism and functions. Immunity 32(5):593-604.

Harayama T, Eto M, Shindou H, Kita Y, Otsubo E, Hishikawa D, Ishii S, Sakimura K, Mishina M, Shimizu T. 2014. Lysophospholipid acyltransferases mediate phosphatidylcholine diversification to achieve the physical properties required in vivo. Cell metabolism 20(2):295-305.

Hishikawa D, Hashidate T, Shimizu T, Shindou H. 2014. Diversity and function of membrane glycerophospholipids generated by the

remodeling pathway in mammalian cells. J Lipid Res 55(5):799-807.

Hishikawa D, Shindou H, Kobayashi S, Nakanishi H, Taguchi R, Shimizu T. 2008. Discovery of a lysophospholipid acyltransferase family essential for membrane asymmetry and diversity. Proceedings of the National Academy of Sciences of the United States of America 105(8):2830-2835.

Holzer RG, Park EJ, Li N, Tran H, Chen M, Choi C, Solinas G, Karin M. 2011. Saturated fatty acids induce c-Src clustering within membrane subdomains, leading to JNK activation. Cell 147(1):173-184.

Ishibashi M, Varin A, Filomenko R, Lopez T, Athias A, Gambert P, Blache D, Thomas C, Gautier T, Lagrost L, Masson D. 2013. Liver X receptor regulates arachidonic acid distribution and eicosanoid release in human macrophages: a key role for lysophosphatidylcholine acyltransferase 3. Arterioscler Thromb Vasc Biol 33(6):1171-1179.

Ishii M, Wen H, Corsa CA, Liu T, Coelho AL, Allen RM, Carson WFt, Cavassani KA, Li X, Lukacs NW, Hogaboam CM, Dou Y, Kunkel SL. 2009. Epigenetic regulation of the alternatively activated macrophage phenotype. Blood 114(15):3244-3254.

Ishii S, Shimizu T. 2000. Platelet-activating factor (PAF) receptor and genetically engineered PAF receptor mutant mice. Prog Lipid Res 39(1):41-82.

Ishiyama J, Taguchi R, Akasaka Y, Shibata S, Ito M, Nagasawa M, Murakami K. 2011. Unsaturated FAs prevent palmitate-induced

LOX-1 induction via inhibition of ER stress in macrophages. J Lipid Res 52(2):299-307.

Jaguin M, Houlbert N, Fardel O, Lecureur V. 2013. Polarization profiles of human M-CSF-generated macrophages and comparison of M1-markers in classically activated macrophages from GM-CSF and M-CSF origin. Cellular immunology 281(1):51-61.

Jain S, Zhang X, Khandelwal PJ, Saunders AJ, Cummings BS, Oelkers P. 2009. Characterization of human lysophospholipid acyltransferase 3. J Lipid Res 50(8):1563-1570.

Kanda Y. 2013. Investigation of the freely available easy-to-use software 'EZR' for medical statistics. Bone marrow transplantation 48(3):452-458.

Kazachkov M, Chen Q, Wang L, Zou J. 2008. Substrate preferences of a lysophosphatidylcholine acyltransferase highlight its role in phospholipid remodeling. Lipids 43(10):895-902.

Kennedy EP, Weiss SB. 1956. The function of cytidine coenzymes in the biosynthesis of phospholipids. The Journal of biological chemistry 222(1):193-214.

Kremer AE, Martens JJ, Kulik W, Rueff F, Kuiper EM, van Buuren HR, van Erpecum KJ, Kondrackiene J, Prieto J, Rust C, Geenes VL, Williamson C, Moolenaar WH, Beuers U, Oude Elferink RP. 2010. Lysophosphatidic acid is a potential mediator of cholestatic pruritus. Gastroenterology 139(3):1008-1018.

Kurabe N, Hayasaka T, Ogawa M, Masaki N, Ide Y, Waki M, Nakamura T, Kurachi K, Kahyo T, Shinmura K, Midorikawa Y, Sugiyama Y, Setou M, Sugimura H. 2013. Accumulated phosphatidylcholine (16:0/16:1) in human colorectal cancer; possible involvement of LPCAT4. Cancer science 104(10):1295-1302.

Lands WEM. 1958. Metabolism of glycerolipides: a comparison of lecithin and triglyceride synthesis. The Journal of biological chemistry 231(2):883-888.

Martinez FO, Gordon S, Locati M, Mantovani A. 2006. Transcriptional profiling of the human monocyte-to-macrophage differentiation and polarization: new molecules and patterns of gene expression. The Journal of Immunology 177(10):7303-7311.

Morita Y, Sakaguchi T, Ikegami K, Goto-Inoue N, Hayasaka T, Hang VT, Tanaka H, Harada T, Shibasaki Y, Suzuki A, Fukumoto K, Inaba K, Murakami M, Setou M, Konno H. 2013. Lysophosphatidylcholine acyltransferase 1 altered phospholipid composition and regulated hepatoma progression. Journal of hepatology 59(2):292-299.

Mosmann TR, Coffman RL. 1989. TH1 and TH2 cells: different patterns of lymphokine secretion lead to different functional properties. Ann Rev Immunol 7:145-173.

Muller-Quernheim UC, Potthast L, Muller-Quernheim J, Zissel G. 2012. Tumor-cell co-culture induced alternative activation of macrophages is modulated by interferons in vitro. Journal of interferon & cytokine

research : the official journal of the International Society for Interferon and Cytokine Research 32(4):169-177.

Nakanishi H, Shindou H, Hishikawa D, Harayama T, Ogasawara R, Suwabe A, Taguchi R, Shimizu T. 2006. Cloning and characterization of mouse lung-type acyl-CoA:lysophosphatidylcholine acyltransferase 1 (LPCAT1). Expression in alveolar type II cells and possible involvement in surfactant production. The Journal of biological chemistry 281(29):20140-20147.

Pelegrin P, Surprenant A. 2009. Dynamics of macrophage polarization reveal new mechanism to inhibit IL-1beta release through pyrophosphates. The EMBO journal 28(14):2114-2127.

Porcheray F, Viaud S, Rimaniol AC, Leone C, Samah B, Dereuddre-Bosquet N, Dormont D, Gras G. 2005. Macrophage activation switching: an asset for the resolution of inflammation. Clin Exp Immunol 142(3):481-489.

Prieur X, Mok CYL, Velagapudi VR, Núñez V, Fuentes L, Montaner D, Ishikawa K, Camacho A, Barbarroja N, O'Rahilly S, Sethi JK, Dopazo J, Oresic M, Ricote M, Vidal-Puig A. 2011. Differential lipid partitioning between adipocytes and tissue macrophages modulates macrophage lipotoxicity and M2/M1 polarization in obese mice. Diabetes 60(3):797-809.

Rong X, Albert CJ, Hong C, Duerr MA, Chamberlain BT, Tarling EJ, Ito A, Gao J, Wang B, Edwards PA, Jung ME, Ford DA, Tontonoz P. 2013.

LXRs regulate ER stress and inflammation through dynamic modulation of membrane phospholipid composition. Cell metabolism 18(5):685-697.

Sanchez-Reyes K, Bravo-Cuellar A, Hernandez-Flores G, Lerma-Diaz JM, Jave-Suarez LF, Gomez-Lomeli P, de Celis R, Aguilar-Lemarroy A, Dominguez-Rodriguez JR, Ortiz-Lazareno PC. 2014. Cervical cancer cell supernatants induce a phenotypic switch from U937-derived macrophage-activated M1 state into M2-like suppressor phenotype with change in Toll-like receptor profile. BioMed research international 2014:683068.

Shea TB, Beermann ML. 1994. Respective roles of neurofilaments, microtubules, MAP1B, and tau in neurite outgrowth and stabilization. Mol Biol Cell 5(8):863-875.

Shindou H, Hishikawa D, Harayama T, Yuki K, Shimizu T. 2009. Recent progress on acyl CoA: lysophospholipid acyltransferase research. J Lipid Res 50 Suppl:S46-51.

Shindou H, Hishikawa D, Nakanishi H, Harayama T, Ishii S, Taguchi R, Shimizu T. 2007. A single enzyme catalyzes both platelet-activating factor production and membrane biogenesis of inflammatory cells. Cloning and characterization of acetyl-CoA:Lyso-PAF acetyltransferase. The Journal of biological chemistry 282(9):6532-6539.

Sica A, Mantovani A. 2012. Macrophage plasticity and polarization: in vivo

veritas. The Journal of clinical investigation 122(3):787-795.

Snyder F. 1989. Biochemistry of platelet-activating factor: a unique class of biologically active phospholipids. Proc Soc Exp Biol Med 190(2):125-135.

Solinas G, Germano G, Mantovani A, Allavena P. 2009. Tumor-associated macrophages (TAM) as major players of the cancer-related inflammation. Journal of leukocyte biology 86(5):1065-1073.

Stein M, Keshav S, Harris N, Gordon S. 1992. Interleukin 4 potently enhances murine macrophage mannose receptor activity: a marker of alternative immunologic macrophage activation. The Journal of experimental medicine 176(1):287-292.

Tjiu JW, Chen JS, Shun CT, Lin SJ, Liao YH, Chu CY, Tsai TF, Chiu HC, Dai YS, Inoue H, Yang PC, Kuo ML, Jee SH. 2009. Tumor-associated macrophage-induced invasion and angiogenesis of human basal cell carcinoma cells by cyclooxygenase-2 induction. The Journal of investigative dermatology 129(4):1016-1025.

Umemura N, Saio M, Suwa T, Kitoh Y, Bai J, Nonaka K, Ouyang GF, Okada M, Balazs M, Adany R, Shibata T, Takami T. 2008. Tumor-infiltrating myeloid-derived suppressor cells are pleiotropic-inflamed monocytes/macrophages that bear M1- and M2-type characteristics. Journal of leukocyte biology 83(5):1136-1144.

Vereyken EJ, Heijnen PD, Baron W, de Vries EH, Dijkstra CD, Teunissen CE. 2011. Classically and alternatively activated bone marrow derived

macrophages differ in cytoskeletal functions and migration towards specific CNS cell types. Journal of neuroinflammation 8:58.

Yamamoto H, Naito Y, Okano M, Kanazawa T, Takematsu H, Kozutsumi Y. 2011. Sphingosylphosphorylcholine and lysosulfatide have inverse regulatory functions in monocytic cell differentiation into macrophages. Arch Biochem Biophys 506(1):83-91.

Zhang F, Liu H, Jiang G, Wang H, Wang X, Wang H, Fang R, Cai S, Du J. 2015. Changes in the proteomic profile during the differential polarization status of the human monocyte-derived macrophage THP-1 cell line. Proteomics 15(4):773-786.

Zhao Y, Chen YQ, Bonacci TM, Bredt DS, Li S, Bensch WR, Moller DE, Kowala M, Konrad RJ, Cao G. 2008. Identification and characterization of a major liver lysophosphatidylcholine acyltransferase. The Journal of biological chemistry 283(13):8258-8265.

Figure legends

Fig. 1 PMA promotes the differentiation of human U937 monocytic cells into macrophage-like cells

U937 cells (5×10^5 cells/well) were seeded into 6-well plates and treated with DMSO or PMA (100 ng/ml) for 12 h.

A: Representative images of DMSO-treated U937 cells (DMSO) and PMA-treated U937 cells (PMA). Scale bar = 50 μm.

B: The mRNA expression of the macrophage differentiation marker CD68 was analyzed by quantitative real-time PCR. Data are presented as the mean ± SD of three independent experiments. $*p < 0.01$ vs. DMSO.

C: Phagocytic activity was measured by flow cytometry. Filled and unfilled histograms represent DMSO-treated U937 cells (DMSO) and PMA-treated U937 cells (PMA), respectively. The experiment was performed three times. Similar results were obtained for each experiment and a representative histogram is shown.

Fig. 2 LPS and IL-4 alter the morphology and function of PMA-treated U937 cells

U937 cells (5×10^5 cells/well) were seeded into 6-well plates and treated with PMA (100 ng/ml) for 12 h. After washing with PBS, the samples were stimulated with LPS (100 ng/ml) or IL-4 (20 ng/ml) for various periods of time (12, 24, 48 and 72 h).

A: Representative images of M1- and M2-polarized macrophages (*upper*). Scale bar = 50 μm. The percentage of spindle-shaped cells (positive cells) was quantified as described in the materials and methods section (*lower*). $*p < 0.01$ vs. IL-4.

B: Phagocytic activity was measured by flow cytometry. Filled, black, red and blue histograms represent DMSO-treated U937 cells (DMSO), PMA-treated U937 cells (Control), LPS-activated U937 cells (LPS) and IL-4-activated U937 cells (IL-4), respectively. The experiment was performed three times. Similar results were obtained for each experiment and a representative histogram is shown.

Data are presented as the mean ± SD of three independent experiments.

Fig. 3 LPS induces the expression of M1 markers

A, B and C: The mRNA expression of the M1 macrophage markers CXCL10, TNF-α, and IL-1β was analyzed by quantitative real-time PCR. $*p < 0.01$ vs. LPS at 0 h (*left panels*). The secretion of CXCL10 and TNF-α in culture after 72 h was analyzed by ELISA. $^{\#}p < 0.01$ vs. control, $*p < 0.01$ vs. IL-4 (A and B, *right panels*). The protein expression of IL-1β was analyzed by western blotting. The experiment was performed three times. Similar results were obtained for each experiment and a representative immunoblot is shown (C, *right*).

Fig. 4 IL-4 induces the expression of M2 markers

A, B and C: The expression of M2 macrophage markers CD206, IL-1ra and TGF-β was analyzed by quantitative real-time PCR. $^{\#}p < 0.01$ vs. IL-4 at 0 h (*left panels*). The protein expression of CD206 and IL-1ra was analyzed by western blotting. The experiment was performed three times. Similar results were obtained for each experiment and representative immunoblots are shown (A, *middle* and B, *right panels*). CD206 membrane expression was measured by flow cytometry. Filled and black histograms represented DMSO-treated U937 cells (DMSO) and IL-4-activated U937

cells (IL-4), respectively. The experiment was performed three times. Similar results were obtained for each experiment and a representative histogram is shown (A, *right*). The secretion of TGF-β in culture after 72 h was analyzed by ELISA (C, *right*).

Fig. 5 LPS significantly decreases the mRNA expression of LPCATs and their enzymatic activities

A: The mRNA expression of LPCAT1, LPCAT2, LPCAT3 and LPCAT4 was analyzed by quantitative real-time PCR. $^{*}p < 0.01$ vs. LPS at 0 h. $^{\#}p < 0.01$ vs. IL-4 at 0 h.

B: LPCAT activity was measured using LC-MS/MS. $^{\#}p < 0.01$ vs. control, $^{*}p < 0.01$ vs. IL-4.

Data are presented as the mean ± SD of three independent experiments.

DPPC, dipalmitoyl phosphatidylcholine; POPC, palmitoyl oleoyl phosphatidylcholine; PLPC, palmitoyl linoleoyl phosphatidylcholine; PAPC, palmitoyl arachidonoyl phosphatidylcholine; PDPC, palmitoyl docosahexaenoyl phosphatidylcholine.

Fig. 6 Knockdown of LPCAT3 in PMA-treated U937 cells decreases LPCAT activity toward linoleoyl-CoA and arachidonoyl-CoA

U937 cells (5×10^5 cells/well) were seeded into 6-well plates and treated with PMA (100 ng/ml) for 12 h. After washing with PBS, the samples were transfected with control siRNA (siControl) and LPCAT3 siRNA (siLPCAT3) using Lipofectamine® RNAi MAX and incubated for 48 h.

A: The mRNA expression of LPCAT3 was analyzed by quantitative real-time PCR.

B: LPCAT activity was measured using LC-MS/MS.

Data are presented as the mean ± SD of three independent experiments. $^{*}p < 0.01$ vs.

control siRNA-transfected cells.

Fig. 7 Knockdown of LPCAT3 shifts PMA-treated U937 cells from M2- to M1-polarized macrophages

A: Representative images of control siRNA (siControl) and LPCAT3 siRNA (siLPCAT3) in PMA-treated U937 cells (*left panels*). Scale bar = 50 μm. The percentage of spindle-shaped cells was quantified as described in the materials and methods section (*right*). $*p < 0.01$ vs. control siRNA-transfected cells.

B: U937 cells (5×10^5 cells/well) were seeded into 6-well plates and treated with PMA (100 ng/ml) for 12 h. After washing with PBS, the samples were transfected with control siRNA and LPCAT3 siRNA for 24 h. The cells were rinsed with 2 ml of RPMI supplemented with 5% FBS and then stimulated with or without IL-4 (20 ng/ml) and incubated for 48 h. The secretion of CXCL10 was analyzed by ELISA. Data are presented as the mean ± SD of three independent experiments. $*p < 0.01$ vs. control siRNA-transfected cells with IL-4 at 48 h.

C: CD206 protein expression was analyzed by western blotting. The experiment was performed three times. Similar results were obtained for each experiment and a representative immunoblot is shown. Band intensity levels were normalized to β-actin. Data are presented as the mean ± SD of three independent experiments. $*p < 0.01$ vs. LPCAT3 siRNA-transfected cells stimulated with IL-4.

Fig. 1

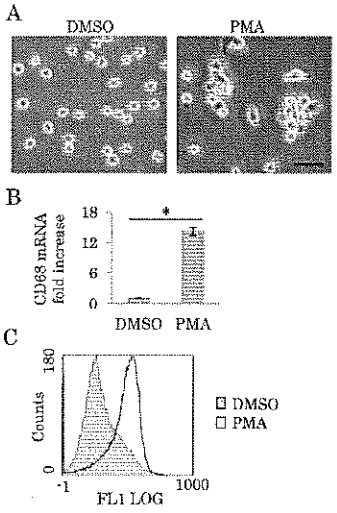

190x254mm (300 x 300 DPI)

Fig. 2

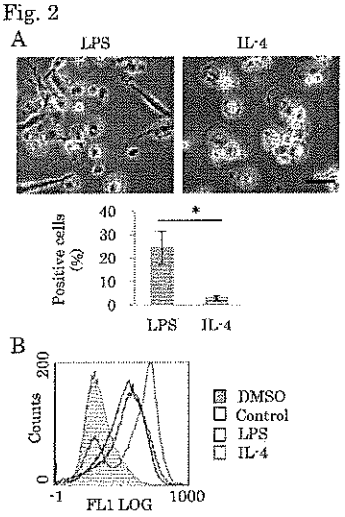

190x254mm (300 x 300 DPI)

Fig. 3

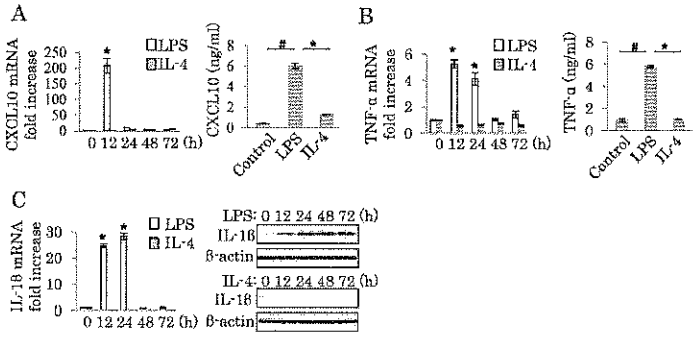

190x254mm (300 x 300 DPI)

Fig. 4

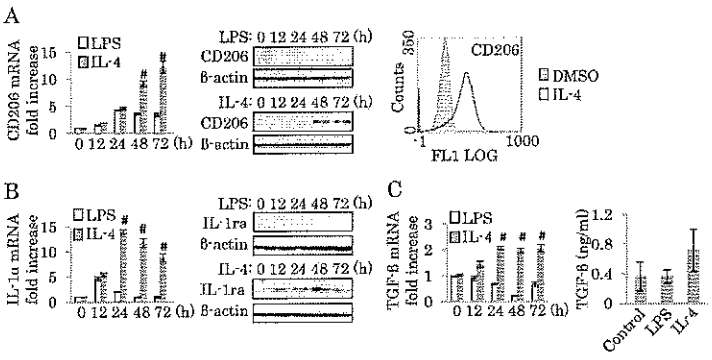

190x254mm (300 x 300 DPI)

Fig. 5

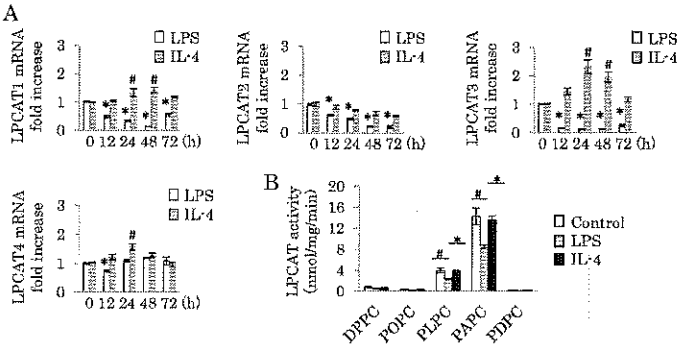

190x254mm (300 x 300 DPI)

Fig. 6

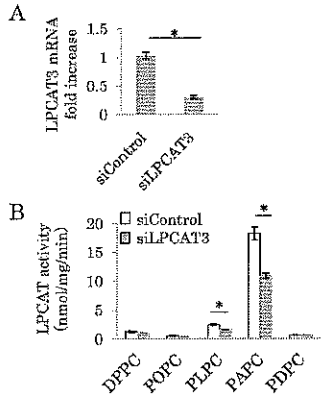

190x254mm (300 x 300 DPI)

Fig. 7

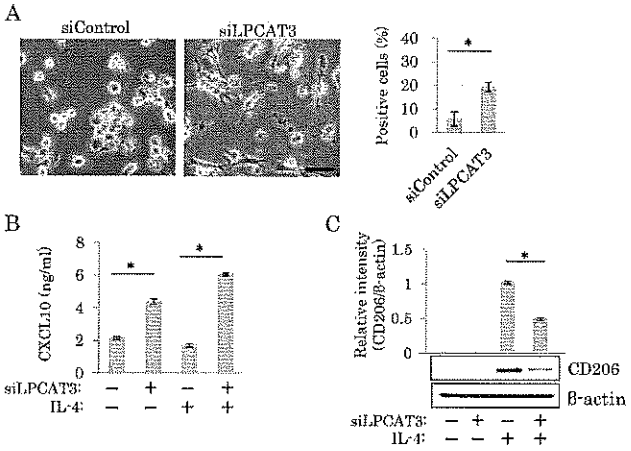

190x254mm (300 x 300 DPI)

Table1. The sequences of the primer pairs used in this analysis are indicated.

Name	Sense primer, 5'→3'	Antisense primer, 5'→3'
18S rRNA	CGAACGTCTGCCCTATCAACTT	ACCCGTGGTCACCATGGTA
CD68	AGGCTGTGGGTGGGATCA	CTTGGAAAGGAGGAAATGAAAGTC
CXCL10	TTCCTGCAAGCCAATTTTGTC	TCTTCTCACCCTTCTTTTTCATTGT
CD206	CGCTACTAGGCAATGCCAATG	GCAATCTGCGTACCACTTGTTTT
TNF-α	GCAGGTCTACTTTGGGATCATTG	GCGTTTGGGAAGGTTGGA
IL-1β	TCAGCCAATCTTCATTGCTCAA	TGGCGAGCTCAGGTACTTCTG
TGF-β	CGCGTGCTAATGGTGGAAA	GCTGTGTGTACTCTGCTTGAACTTGT
IL-1ra	CTGCACAGCGATGGAAGCT	GCCTTCGTCAGGCATATTGG
LPCAT1	TTGCTTCCAATTCGTGTCTTATT	ATCCCATTGAAAAGAACATAGCA
LPCAT2	CCTCATGACACTGACGCTCTTC	CAGGAAGTCCACAACCTTCCTC
LPCAT3	CATTGCCTCATTCAACATCAACA	AGGAATTCCATCTGGAAGCAGAC
LPCAT4	AAGGTGGCGTTGGAACCA	CCCAGCCTTCCGAAGCA